ICSV14
Cairns • Australia
9-12 July, 2007

14th International Congress on Sound & Vibration

PREDICTIONS OF FAN BROADBAND NOISE DUE TO ROTOR-STATOR INTERACTION

Vincent Jurdic[1 *], Phillip Joseph[1 †], Antoine Moreau[2 ‡], Lars Enghardt[2 §]

[1]ISVR
University of Southampton
University road
Southampton SO17
England

[2]German Aerospace Center (DLR)
Institute of Propulsion Technology, Engine Acoustics Branch
Mueller-Breslau-Str. 8
10623 Berlin
Germany

[*]vj@isvr.soton.ac.uk
[†]pfj@isvr.soton.ac.uk
[‡]antoine.moreau@dlr.de
[§]lars.enghardt@dlr.de

Abstract

This paper presents a comparison of the predicted and measured broadband noise generated in a low-speed fan rig. It is assumed that the dominant noise generation mechanism is rotor-stator interaction whereby turbulent wakes from the rotor interact with the downstream stator.

The stator is modelled as a cascade of flat plate airfoils. The acoustic response of these blades is predicted using classical theory for the acoustic response due a rectilinear cascade of flat plate airfoils in which a harmonic (single-frequency,single-wavenumber) gust is incident. This theory has been extended to predict the broadband noise generated by impinging homogenous isotropic turbulence. The present paper proposes a comparison between measured and predicted noise power spectra.

Aerodynamic measurements have also been performed at different radial positions downstream of the rotor to obtain velocity spectra and wake profiles.

The aerodynamics measurements will be presented in this paper to validate the assumptions of homogenous isotropic turbulence made in the noise model. From these measurements, the turbulence intensity and length scale at the stator leading edge are also determined as input quantities to the noise model.

1. INTRODUCTION

Improvements in the reduction of jet noise and fan tones have meant that fan broadband noise is now a major noise source. It is widely believed that the dominant source of fan broadband noise is due to the interaction between rotor wake turbulence and the stator vanes.

The first part of this paper deals with the formulation of Cheong et al [1] for the acoustic power spectrum radiated by a two-dimensional flat plate cascade due to impinging isotropic homogeneous turbulence. The second part of this paper describes the experimental low speed fan rig at DLR Berlin. The third part of this paper describes the aerodynamic and acoustic measurements for the use in the prediction model. Finally, a comparison is presented between the measured and predicted sound power spectra, upstream and downstream of the fan stage.

2. ROTOR-STATOR INTERACTION BROADBAND NOISE MODEL

The broadband noise generated by rotor-stator interaction is predicted based on strip theory applied to the stator. The sound power radiated by each strip is predicted using a two-dimensional model of the unsteady blade response. Justification for the use of a two-dimensional blade response model follows from the findings by Cheong et al [1] in which noise predictions obtained using the current two-dimensional model gave near identical results to that obtained using the three-dimensional noise model of Hanson [2]. Each section is unrolled at the mid-section radius to produce an infinite cascade of flat plates of chord c, spaced by s and with a stagger angle θ as shown in figure 1. The coordinate systems (x_1, x_2, x_3) corresponds to a unrolled duct-bound coordinate system while (y_1, y_2, y_3) is a vane-bound coordinate system with y_1 being in the chordwise direction. The cascade is immersed in a mean flow of speed U_1 in the direction of the stator. Velocity fluctuations are assumed to be very small compared to the mean velocity magnitude U_1. The two-dimensional model also assumes that the flat plate cascade is situated in a free-field and that the duct has no effect on the sound power radiation.

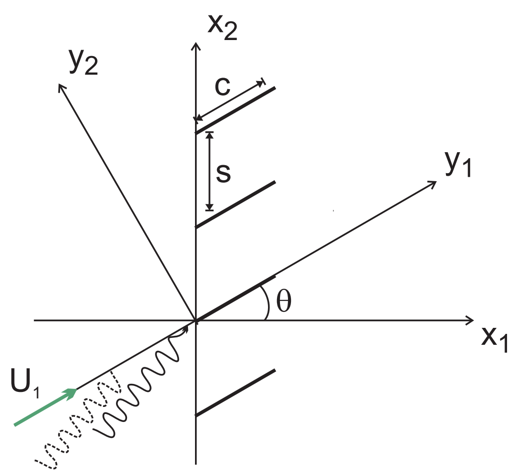

Figure 1. Cascade model and coordinate system

An expression for the sound power has been formulated in which an infinite number of impinging vortical Fourier modes interacts with the cascade, each of which is scattered into an infinite sum of acoustic modes. The vortical and acoustic mode indices m and l are related by the scattering rule:

$$l = m - Vr \tag{1}$$

where V is the number of stator vanes and r is a scattering index, ranging from $-\infty$ to ∞.

The spectral density of sound power per unit span $\mathfrak{P}^{\pm}$ may also be expressed as the double summation [1]:

$$\mathfrak{P}^{\pm}(\omega) = \frac{2\pi\rho_0 M}{\cos\theta} \sum_{l=-\infty}^{\infty} Q_l^{\pm}(K_1, k_{2,l}) \sum_{r=-\infty}^{\infty} \Phi_{ww}(K_1, k_{2,l+Br}) \tag{2}$$

where the turbulence wavenumber $k_{2,l}$ is given by:

$$k_{2,l} = \frac{2\pi}{V s \cos\theta} l - K_1 \tan\theta \tag{3}$$

$Q_l^{\pm}$ is the modal power response function which specifies the non-dimensional modal power due to the r^{th} cascade wave excited by a vortical gust. The details of these functions are given in Cheong et al [1]. The response function $Q_r^{\pm}$ is completely determined by the solidity s/c, the stagger angle θ, the Mach number M, the reduced frequency $K_1 c = \omega c/U_1$ and the number of stator vanes V. The term $\Phi_{ww}(k_1, k_2)$ is the two-dimensional energy spectrum of the fluctuating velocity component normal to the chord.

2.1. Turbulence spectrum

In this paper, for simplicity, the rotor wake turbulence impinging on the stator vanes is assumed to be axi-symmetric, isotropic and homogeneous. Justification for this simplistic turbulence model can be found in figure 4 in which high levels of background turbulence are observed. By contrast, the the wakes occur over a much smaller region with turbulence levels that are not significantly greater than the background levels. A more detailled turbulence model that includes the details of the wake is proposed by jurdic et al.[3]. Two analytical formulations are available to express this energy spectrum: the Liepmann model and the von Karman model [4]. The important difference between the models is the high frequency rate of decay of K_1^{-3} and $K_1^{-8/3}$ for the Liepmann's and von Karman's formulation, respectively. In this paper, the sound power spectra have been predicted using only the Liepmann model as only small differences in the predicted sound power spectra were found between the two turbulence models.

The two-dimensional energy spectrum is expressed using Liepmann's model by:

$$\Phi_{ww}(k_1, k_2) = \frac{\overline{u_2^2}\Lambda^2}{4\pi} \frac{1 + \Lambda^2(4k_1^2 + k_2^2)}{(1 + \Lambda^2(k_1^2 + k_2^2))^{5/2}} \tag{4}$$

where Λ is the turbulence length scale and $\overline{u_2^2}$ is the mean square value of the velocity fluctuation perpendicular to the stator chord.

3. LOW SPEED FAN RIG

DLR in Berlin, Germany, has performed extensive aerodynamic and acoustic measurements in a low-speed fan rig. The fan stage consists of a 24-blade rotor and a 16-vane stator. The stator vanes correspond to an arc of a circle of radius $139.4\ mm$. The trailing edge angle is constant and equal to -6.3^o, the leading edge angle decreases linearly from 42.8^o at the hub to 36.9^o at the tip. The stator span is $87.7\ mm$ in length which gives a hub and tip radius equal to $R_{hub} = 138.8\ mm$ and $R_{tip} = 226.5\ mm$, respectively. Figure 2 shows the location of the various transducers on the rig. A summary of the transducers and their purpose is listed below:

- The fan performance characteristics are obtained by static wall pressure measurements, positioned downstream and upstream of the fan stage.
- Microphone arrays are located near the inlet of the duct as well as downstream of the fan stage. The inlet array consisted of 23 wall-flush mounted microphones, although the downstream array of sensors was arranged in radial rakes with 8 microphones.
- 2-components hot-wire probes were used to measure the velocity in the inlet and in the inter-stage section.
- Unsteady pressure sensors inside the rotor blades and stator vanes have employed to determine the surface pressure spectrum.

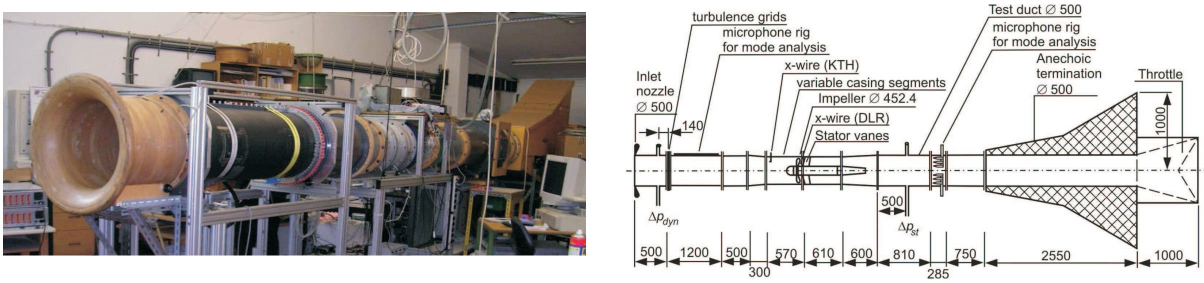

Figure 2. Photograph (left) and schematic overview (right) of the DLR-Berlin fan rig with instrumentation.

Comparisons of the measured and predicted power spectra presented in this paper correspond to a rotor blade tip clearance of 0.6mm, an inlet Mach number of 0.04, a pressure ratio of 1.014, and a rotor speed of 3220rpm, which corresponds to a blade tip Mach number of 0.22.

Aerodynamic measurements were made at two axial positions between the fan and the stator. The interstage aerodynamics measurements were made using 2-components hot-wire probes located at 2 different axial positions of $x_1 = 63\ mm$ and $x_2 = 115\ mm$ from the hub rotor trailing edge. For each axial position, measurements were made at 40 non linearly spaced radial positions. The measurement positions near the hub and the tip are separated closer than in the mid span region to resolve the wall boundary layers. A tacho pulse related to the shaft rotation frequency is extracted to provide a phase reference for the measurements. The measurements made over one full rotation are then discretised into 936 equispaced points, leading to 39 points between 2 blades, giving a circumferential resolution of 0.38^o. All the measured flow quantities have been averaged over 200 rotations.

4. INTERSTAGE AERODYNAMIC MEASUREMENTS

The aerodynamic input data required by the noise model is obtained directly from the interstage measurements. Details of these aerodynamic measurements are presented below.

The mean velocity components in the vane-fixed coordinate system (y_1, y_2, y_3) are plotted in figure 3 as a contour map. As expected, the velocity component in the stator direction, U_1, is seen to be almost constant along any given radius, especially in the mid span region. Near the hub and tip wall regions, small variations in velocity can be observed. The two velocity components normal to the chord, U_2 and U_3, exhibit strong periodicity, showing the presence of the rotor wakes. In the mid span region the rotor wakes are thin compared to the distance between adjacent blades but much thicker at the tip and hub regions. In the near wall regions, the mean velocity is affected, not only by rotor wakes, but also by wall boundary layers and secondary flows. Outside the rotor wakes and the tip and hub regions U_2 and U_3 are relatively small compared to U_1. These measurements confirm that the mean flow impinges upon the stator with an angle of attack equal to zero. Furthermore the radial components of the flow can be neglected. Both of these findings are consistent with assumptions in the model.

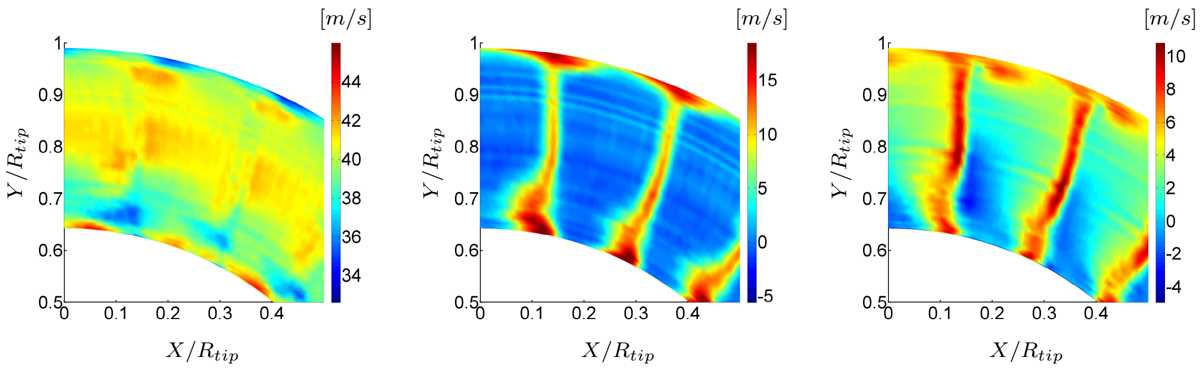

(a) Mean velocity component U_1 (b) Mean velocity component U_2 (c) Mean velocity component U_3

Figure 3. Contour map of the mean velocity components in the stator coordinate system at the position x_2

Figure 4 (a) represents, at position x_2, a contour map of Tu, the local turbulence kinetic energy normalised by the mean velocity amplitude of the flow, defined by:

$$Tu = \sqrt{\frac{\frac{1}{2}\left(\overline{u_1^2} + \overline{u_2^2} + \overline{u_3^2}\right)}{U_1^2 + U_2^2 + U_3^2}} \tag{5}$$

In figure 4 (b) the circumferential profiles of Tu at position x_2 is plotted for different radial positions: the continuous curve is near the hub at 7.7% of the span, the dashed curve is in the mid span at 50.4% and the dotted curve is in the tip region at 97.5%.

The rotor wakes are clearly visible, with a maximum $Tu-$value of about 8%, confined over a narrow range of pitch angles. Between the wakes, the value of Tu is approximately equal to 2%, which is roughly the same levels as the turbulence ingested by the rotor. High values of Tu can be seen close to the wall in the hub and tip regions. Differences between the rotor blades are also clearly visible, especially due to the secondary flow generated near the hub.

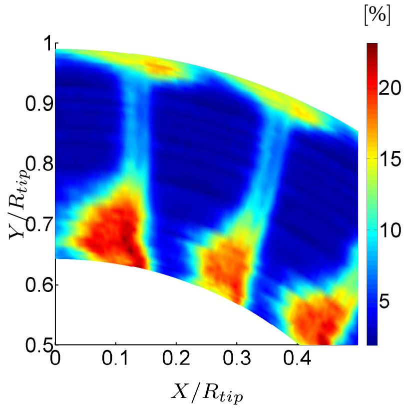

(a) Contour map of Tu

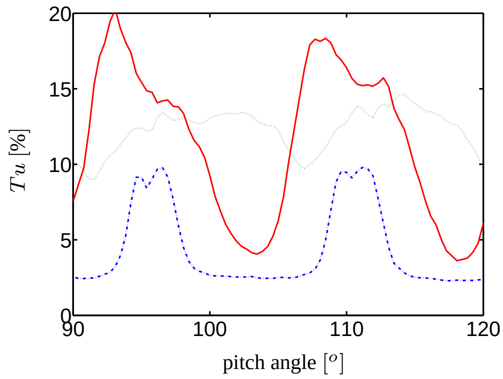

(b) Circumferential profiles of Tu

Figure 4. Contour map (a) and circumferential profiles (b) of Tu for 7.7% (——), 50.4% (- - - -) and 97.5% (· · · · ·) of the span, at the axial position x_2

In this paper the turbulence model is completly defined by a the mean square value of the velocity $\overline{u_2^2}$ and length scale Λ. The turbulence length scale is deduced from the work of Ganz et al [6], which showed from measurement in a low speed fan rig that the turbulence length scale is approximately 40% of the half wake width L_0. While $\overline{u_2^2}$ is deduced from the averaged over the circumference.

Figure 4shows that in the mid-span region, the rotor wake is clearly defined and a value for L_0 is readly obtained. However, near the walls, defining L_0 is more difficult because of the wall and secondary flow effects. Figure 5(a) and (b) show the turbulence intensity and length scale, respectively, plotted against the 40 radial measurement points along the span.

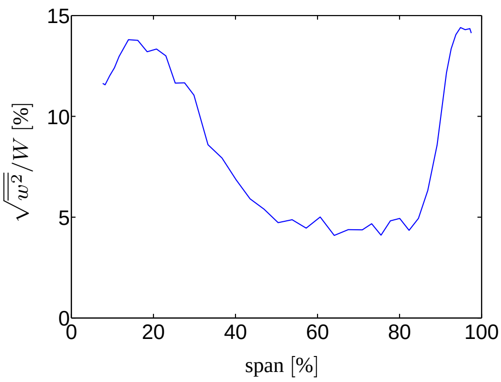

(a) Turbulence intensity

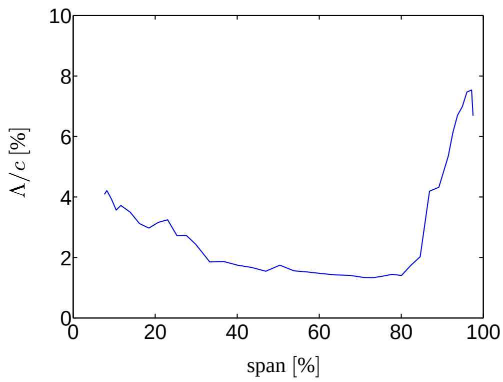

(b) Turbulence length scale

Figure 5. Cirumferentially averaged turbulence intensity (a) and length scale (b) versus the span at the position x_2

Figure 5(a) reveals that the turbulence intensity profile can be divided into three distinct regions. Near the hub, at approximately 35% of the span, the turbulence intensity is high because of strong secondary flow behind the rotor blades. Near the tip, at around 80% of the span, the turbulence intensity and length scale increase rapidly. In the mid span region the turbulence intensity and length scale are much lower. Despite the presence of wakes, the $Tu-$value averaged over the circumference is low because the wake is relatively thin. Thus, the circumferentially averaged Tu includes an important contribution from the turbulence in between the wakes. This finding justifies the use of an axi-symmetric turbulence model. The contribution to the noise from the wakes compared to that in the background flow will be evaluated shortly.

5. COMPARISON BETWEEN MEASURED AND PREDICTED SOUND POWER SPECTRUM

The interstage aerodynamic measurements are performed relatively far from the stator leading edge. Whilst the mean flow velocity can be assumed to be the same at x_2 and at the stator leading edge, the turbulence intensity and length scale must be corrected to take account of spreading by the wake.

Previous studies on rotor wakes by Gliebe et al [5] and Ganz et al [6] show that the turbulence intensity and length scale are roughly proportional to $1/\sqrt{x}$ and $\sqrt{x}$, respectively, in accordance with classical plane wake theory.

A comparison between the measured and predicted upstream and downstream sound power spectra are plotted in figure 6(a) and (b) respectively. The measured sound power spectra are represented by the continuous curve, while the predicted spectra are shown on the dashed curve.

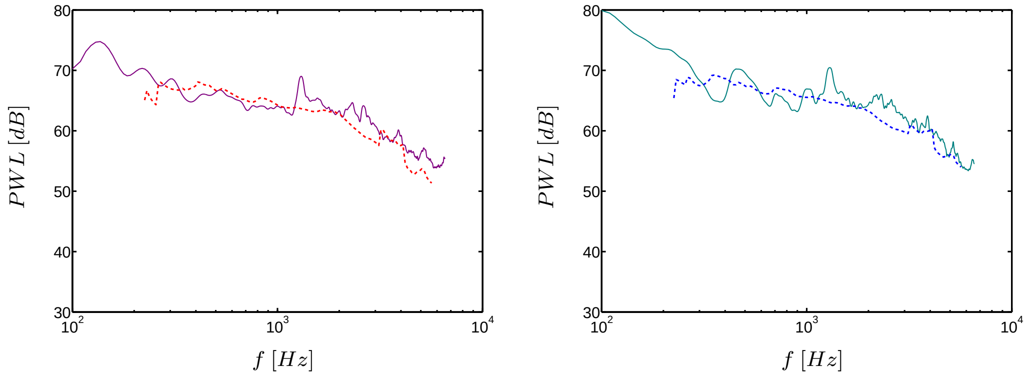

(a) Upstream PWL (b) Downstream PWL

Figure 6. Upstream measured (——) and predicted (- - - -) sound power spectra (a) and downstream measured (——) and predicted (- - - -) sound power spectra (b)

The measured broadband spectra presented in figure 6 have been obtained by frequency filtering the measured sound powe spectra to remove tone noise. The broadband spectra can be seen to be closely predicted by the model. Spectral shape and absolute levels are well predicted, especially the high frequency decay.

6. CONCLUSION

The aerodynamics measurements have shown that the flow impinging upon the stator vanes can be assumed as a uniform two dimensional flow. The flow can be also divided into three distinct regions: the hub, mid span and tip regions. In the mid span region the wakes generate comparatively low levels of turbulence. Near the wall, the turbulence values are larger because of secondary flow and the wall boundary layers.

A simple analytical model of the turbulence impinging the stator vanes has been shown to give encouraging agreement with experimental results. The spectral shape and absolute levels are relatively well predicted.

This preliminary study appears to suggest that most of the broadband noise produced in this low-speed fan rig is generated by secondary flow effects at the walls. More work is needed to confirm this hypothesis.

REFERENCES

[1] C. Cheong, P. Joseph, and S. Lee, "High frequency formulation for the acoustic power spectrum due to cascade-turbulence interaction", *Journal of the Acoustical Society of America* **119**, no. 1, 108–22(2006).

[2] D. B. Hanson, K. P. Horan, "Turbulence/cascade interaction - spectra of inflow, cascade response, and noise", *AIAA/CEAS Aeroacoustics Conference, 4th (19th AIAA Aeroacoustics Conference)*, (June 2-4, 1998).

[3] V. Jurdic, A. Moreau, P. Joseph, L. Enghardt, J. Coupland, "A comparison between measured and predicted fan broadband noise due to rotor-stator interaction", *AIAA/CEAS Aeroacoustics Conference, 13th*, (May 21-23, 2007).

[4] R. K. Amiet, "Acoustic radiation from an airfoil in a turbulent stream", **41**, no. 4, 407–420 (1975). 75120002976.

[5] P. Gliebe, R. Mani,S. Shin, B. Mitchell,G. Ashford,S. Salamah, S. Connell, "Aeroacoustic Prediction Codes", *NASA/CR-2000-210244* (2000).

[6] U. W. Ganz, P. D. Joppa, T. J. Patten, D. F. Scharpf, "Boeing 18-inch fan rig broadband noise test", *NASA/CR-1998-208704* (1998).